Theoretical Modeling and Experimental Validation of Reverse Electrowetting on Dielectric (REWOD) Through Flexible Electrodes For Self-Powered Sensor Applications

Karthik Kakaraparty*, Gretchen S. Hyer[†], Erik A. Pineda*, Russell C. Reid[†] and Ifana Mahbub* *Department of Electrical Engineering, University of North Texas, Texas, USA [†]Department of Engineering, Utah Tech University, Utah, USA.

Abstract—In this paper, theoretical modeling and experimental validation of REWOD energy harvesting based on flexible electrodes for self-powered sensor applications have been investigated. Much of REWOD's research has focused on planar electrodes that have an inflexible, rigid surface and use high bias voltages to increase output power, which undermines the goals of self-powered wearable motion sensors. This article implements REWOD-based energy harvesting using two dissimilar flexible electrodes. Electron beam physical vapor deposition (EBPVD) is used to coat the material onto a polyimide film. A comparative analysis between theoretical model data and experimental measurement data has been conducted.

Index Terms—Energy harvesting, REWOD, flexible electrodes, electrolyte impingement, electro-mechanical modulation.

I. INTRODUCTION

The growing need for self-powered wearable sensors has necessitated the development of energy harvesting systems capable of consistently and sufficiently powering these devices. Within the last decade, among the many ambient energy harvesting technologies that have been developed in recent years are the well-known piezoelectric energy harvesters (PEH), triboelectric nanogenerators (TENG), electromagnetic energy harvesters, and other vibration-based energy harvesters [1]. The lower frequency range (0.25-5 Hz), which is typical for many human motion activities, has been found to be an effective operating range for TENG. Although other energy harvesting technologies have advanced significantly, the majority of them struggle to capture energy in the lowfrequency range (0.25-5 Hz) [2]-[5]. It has been suggested in [6] to use flexible, fiber-based energy harvester (FBH), which incorporate conducting fibers into garments and convert biomechanical vibration energy to electrical energy. Traditional wearable sensors have relied on batteries for power, which reduces the device's longevity, prevent gadget miniaturization and also has certain safety issues like battery explosions and electrolyte leaks [7], [8]. It is essential to develop energy harvesters that are flexible, reliable, and sufficiently power such sensors [9]-[12].

Recently, reverse electrowetting-on-dielectric (REWOD), a novel method of electrostatic energy harvesting, has emerged

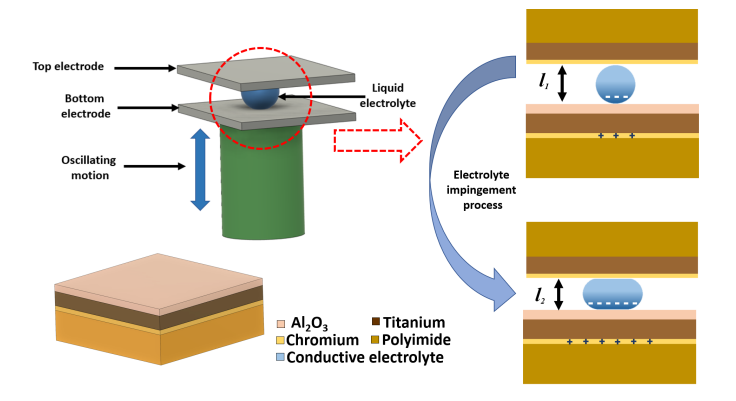


Fig. 1. The principle mechanism of REWOD based energy harvesting without any external bias voltage. The mechanical modulation results in maximum electrodes displacement of $\Delta l = l_1 - l_2$.

in the preceding 10 years. Due to its independence from solid structure resonance, REWOD, unlike many other energy harvesting devices, has been demonstrated to function well at low mechanical frequencies and can be implemented using flexible structures. In REWOD, capacitance from both the electrical double layer (EDL) and the dielectric insulator results in capacitance at the electrode-electrolyte interface. REWOD energy harvesting based on electrolyte impingement is the topic of many recent research works [13]–[25].

The paper is organized as follows: section II presents experimental procedure. Section III presents the theoretical modeling, results and discussion is presented in section IV and the concluding remarks are presented in section V.

II. EXPERIMENTAL SECTION

Two dissimilar electrodes were fabricated using polyimide sheets. A portion of polyimide sheet was cut into two equally sized samples. The first one was coated with chromium (Cr) and titanium (Ti) with coating thicknesses of 50 nm and 150 nm, respectively. The second sample was coated with Cr-50 nm, Ti-150 nm along with the dielectric material Al_2O_3 with coating thickness of 100 nm. The Electron-Beam Physical



Fig. 2. (a) Fabricated flexible electrodes. (b) Flexible bend test sample made with top and bottom electrodes with electrolyte enclosed within the slot made in between 2 electrodes.

Vapor Deposition (EBPVD) technique has been utilized to coat the materials on the polyimide sheet. The aforementioned 3-layer coated sample was used as a bottom electrode and the 2-layer coated sample is used as the top electrode. The coating was visually checked using a trinocular stereo microscope (AmScope 1140) after the completion of the coating process to ensure coating consistency. The conventional REWOD based energy harvesting is as shown in Fig. 1, an electrolyte is placed in between the top and bottom electrodes and the bottom electrode is made to oscillate up and down and as a result the electrolyte impingement takes place facilitating the aforementioned REWOD mechanism.

The bend test sample consists of a bottom electrode attached to a top electrode with double-sided tape and an electrolyte is placed within an enclosed space between the two electrodes. Copper wires are attached to top and bottom electrodes individually and are extended out to facilitate connections for the experimental measurements as shown in the Fig. 2(b). The copper wires attached to the top and bottom electrodes act as collector and ground terminals, respectively. The copper wire is attached to the conductive portion of the bottom electrode using epoxy which is cured for 24 hours as shown in Fig. 3(a), Thick double-sided tape was used to border the bottom electrode and create a support structure to confine the electrolyte as shown in Fig. 3(b). UV-curable adhesive is applied to the entire perimeter of the double-sided tape, and then the adhesive is cured with UV light exposure as shown in Fig. 3(c) to ensure a proper seal. Soon after the glue applied is cured, an electrolyte of 50 µL is used to fill the volume enclosed by the double-sided tape. The coated side of the top electrode is aligned to enclose the space in between both electrodes to complete the seal and for the electrolyte not to leak-out as shown in Fig. 3(d). An additional polyimide sheet is used as a support material for the bend test sample to place on the aforementioned 3D printed structure as shown in Fig. 3(e).

III. THEORETICAL MODELING

This section theoretically shows how liquid surface area changes when the REWOD sample is bent and how this results in electrical current. As shown in Figure 4(b), The REWOD sensor/energy harvester was modeled in 2D, having two arcs of the same length l with endpoints that are a fixed distance d between them. The dimension d_1 is the thickness

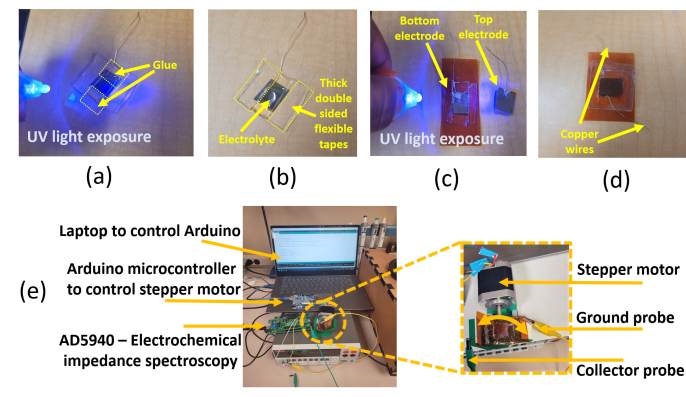


Fig. 3. Implementation of bending test with the actual flexible bend test sample.

of the adhesive that joins the opposing substrates to form the REWOD sensor/harvester. It is assumed that the outer edges of the adhesive remain co-linear with the radius of the outer arc at all times. The arcs are treated as segments of perfect circles. Assuming the outer arc is the driving arc, it has an input bend angle of θ and a resulting radius R with the origin at the center of the driving arc. The driven inner arc is described by its bend angle and radius denoted as ϕ and r, respectively. The arc length, l, radial distance between arcs at their endpoints, d_1 , and the driving angle, θ , are all predetermined. The endpoint coordinates of the outer and inner arcs are as mentioned below:

$$x_{1} = 0 y_{1} = -l/\theta$$

$$x_{2} = -\left(\frac{l}{\theta}\right) * sin(\theta) y_{2} = -\left(\frac{l}{\theta}\right) * cos(\theta)$$

$$x_{3} = 0 y_{3} = -l/\theta + d_{1}$$

$$x_{4} = -\left(\frac{l}{\theta} - d_{1}\right) * sin(\theta) y_{4} = -\left(\frac{l}{\theta} - d_{1}\right) * cos(\theta)$$

$$(1)$$

where the outer arc radius R has been replaced with $\frac{l}{\theta}$ from the equation for arc length $l = R\theta$.

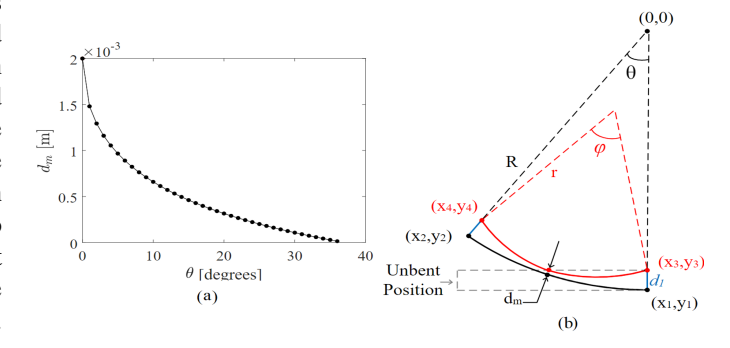


Fig. 4. (a) Distance between inner and outer arcs shown in (b), which represent the two opposing REWOD substrates shown in the unbent position (dashed) and bent at an angle of θ .

The chord lengths for the inner and outer arcs are then found using the distance formula.

$$c_r = \sqrt{(x_4 - x_3)^2 + (y_4 - y_3)^2}$$
 (2)

$$c_R = \sqrt{(x_2 - x_1)^2 + (y_2 - y_1)^2}$$
 (3)

With the chord distances defined, ϕ is determined using trigonometry based on the triangle formed by the inner arc radius, the distance between the center of the inner arc and its chord, and half of the chord length. This results in Equation 4, which can be solved using a root-finding numerical method.

$$sin(\frac{\phi}{2}) = \frac{c_r \phi}{2l} \tag{4}$$

r is defined using the relationship between arc length (l), radius, and angle of bend: $r = l/\phi$. Then, the sagitta of each arc is found as follows:

$$s_r = r - \sqrt{r^2 - \frac{c_r^2}{4}}$$
 $s_R = R - \sqrt{R^2 - \frac{c_R^2}{4}}$ (5)

This makes it possible to define the distance between the arcs with Equation 6. Figure 4(a) shows the distances found from values of θ that were used in the model.

$$d_m = d_1 \cos(\theta) + s_R - s_r \tag{6}$$

The surface area between the electrolyte and the bottom electrode is the electrolyte volume divided by the distance between the arcs: $A_s = volume/d_m$. This approximation neglects the varying gap between the two arcs. With A_s known, it is possible to calculate the voltage output as the bend angle varies. This calculation follows the general procedure detailed in our previous publication [26] with a few modifications as described below. The capacitance is $C = \epsilon_0 \epsilon A_s/d_2$ where ϵ_0 is the permittivity of air and ϵ and ϵ are the relative permittivity and thickness of Al_2O_3 . The equivalent impedance of the REWOD sensor is

$$Z_{eq} = \left(\frac{1}{R_p} + \frac{1}{X_c} + \frac{1}{R_L}\right)^{-1} \tag{7}$$

where R_p is the parallel resistance, R_L is the load resistance, and X_c is the capacitive reactance. The generated voltage across the load is calculated using Equation 8 where V_{dc} is an inherent dc bias voltage at the REWOD surface and $V_{ac} = V_{dc} sin(2\pi ft)$ is the ac component of the REWOD voltage.

$$V = -[(V_{dc} + V_{ac})\frac{dC}{dt} + C\frac{dV_{ac}}{dt}](\frac{X_c}{R_p} + 1 + \frac{X_c}{R_L})Z_{eq}$$
 (8)

 $\label{table I} \textbf{TABLE I}$ Design variables of voltage generation model.

	Specifications	
Variable	Description	Value
Volume	Volume of electrolyte	$50~\mu L$
l	Arc length	16 mm
d_1	Distance between top and bottom electrodes	2 mm
d_2	Thickness of Al_2O_3	100 nm
ε_0	Free-space permittivity	8.85×10 ⁻¹² F/ m ²
ε	Relative permittivity of Al_2O_3	11
R_p	Parallel resistance	383 kΩ*
R_L	Load resistance	11 kΩ*
f	Bending frequency	5 Hz
V_{dc}	Native bias voltage at REWOD interface	10 mV

^{*}Resistance values were determined for [26].

IV. RESULTS AND DISCUSSION

The theoretical time domain voltage plot for one second is presented in Fig. 5(a). The measured data manifested $\approx 30 \text{ mV}$ of dc offset that was also accounted in the theoretical model. The measured time domain plots for the 3 different trials performed are presented in Fig. 5(b). Table 1 summarizes the values used in the theoretical model. The implementation of the bending test with the flexible samples generated a maximum voltage value of 78 mV. The Analog Device impedance and electrochemical front end (AD5940) measured the maximum electrical resistance value of 9.8 M Ω , which is the electrical resistance across the electrodes while the electrolyte enclosed in between them is subjected to impingement process. Using Ohm's law, the maximum estimated current is 7.34 nA at 5 Hz operating frequency and thus resulting in generation of 0.528 μW of power, which is ample enough to power up ultra lowpower bio-wearable chips, which typically would just need nano-watt range of power to activate [27]. The offset in the measured data is due to minute metal electrode impurities and ionic concentration changes that occur as a result of epoxy been used to connect the copper wire and electrode. The model was not capable of predicting this and it was therefore added to the model manually.

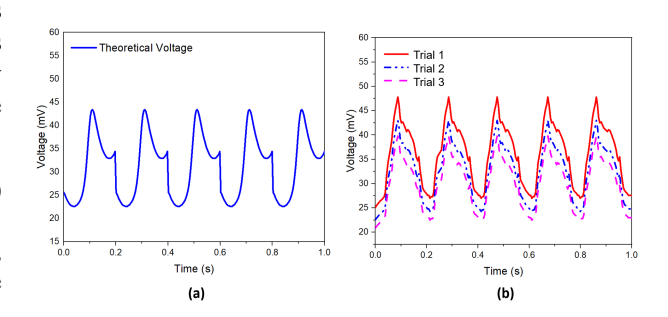


Fig. 5. (a) Theoretical generated voltage plot from a flexible REWOD sensor being repeatedly bent from $\theta=0$ to 30 degrees at 5 Hz. (b) Measured time domain voltage plots at 5Hz for 3 different trials.

V. CONCLUSION

REWOD energy harvesting using flexible electrodes was performed with an objective to demonstrate the power generation without any external bias supply. The voltage generated out of the flexible electrode based REWOD bend test has been modeled and compared with the actual measured voltage data. The theoretical estimation of voltage is in good agreement with the measured data. As a future work, we plan to do more fundamental research into the thickness effect of Al_2O_3 , quantity variation of electrolyte and composite of electrolyte.

ACKNOWLEDGMENT

This work is based upon work supported by the National Science Foundation (NSF) under Grant No. ECCS 1943990.

REFERENCES

- [1] D. Zabek, C. R. Bowen, and J. Taylor, "Electrical capacitance with meshed electrodes for piezo- and pyro-electric energy harvesting applications," in 2015 Joint IEEE International Symposium on the Applications of Ferroelectric (ISAF), International Symposium on Integrated Functionalities (ISIF), and Piezoelectric Force Microscopy Workshop (PFM), 2015, pp. 83–86.
- [2] B. Andò, S. Baglio, V. Marletta, and A. R. Bulsara, "Modeling a nonlinear harvester for low energy vibrations," *IEEE Transactions on Instrumentation and Measurement*, vol. 68, no. 5, pp. 1619–1627, 2019.
- [3] J. J. L. Aranda, S. Bader, and B. Oelmann, "An apparatus for the performance estimation of pressure fluctuation energy harvesters," *IEEE Transactions on Instrumentation and Measurement*, vol. 67, no. 11, pp. 2705–2713, 2018.
- [4] L. Hu, H. Wu, Q. Zhang, H. You, J. Jiao, H. Luo, Y. Wang, A. Gao, and C. Duan, "Self-powered energy-harvesting magnetic field sensor," Applied Physics Letters, vol. 120, no. 4, p. 043902, 2022.
- [5] S. Hu, S. Chang, G. Xiao, J. Lu, J. Gao, Y. Zhang, and Y. Tao, "A stretchable multimode triboelectric nanogenerator for energy harvesting and self-powered sensing," *Advanced Materials Technologies*, vol. 7, no. 3, p. 2100870, 2022.
- [6] J. Zhong, Y. Zhang, Q. Zhong, Q. Hu, B. Hu, Z. L. Wang, and J. Zhou, "Fiber-based generator for wearable electronics and mobile medication," ACS nano, vol. 8, no. 6, pp. 6273–6280, 2014.
- [7] T. Ruan, Z. J. Chew, and M. Zhu, "Energy-aware approaches for energy harvesting powered wireless sensor nodes," *IEEE Sensors Journal*, vol. 17, no. 7, pp. 2165–2173, 2017.
- [8] C. Dagdeviren, Z. Li, and Z. L. Wang, "Energy harvesting from the animal/human body for self-powered electronics," *Annual review of biomedical engineering*, vol. 19, pp. 85–108, 2017.
- [9] J. J. Ruan, R. A. Lockhart, P. Janphuang, A. V. Quintero, D. Briand, and N. de Rooij, "An automatic test bench for complete characterization of vibration-energy harvesters," *IEEE Transactions on Instrumentation and Measurement*, vol. 62, no. 11, pp. 2966–2973, 2013.
- [10] A. Obaid and X. Fernando, "Wireless energy harvesting from ambient sources for cognitive networks in rural communities," in 2017 IEEE Canada International Humanitarian Technology Conference (IHTC), 2017, pp. 139–143.
- [11] M. Ferrari, V. Ferrari, D. Marioli, and A. Taroni, "Modeling, fabrication and performance measurements of a piezoelectric energy converter for power harvesting in autonomous microsystems," *IEEE Transactions on Instrumentation and Measurement*, vol. 55, no. 6, pp. 2096–2101, 2006.
- [12] C. Xu, Y. Song, M. Han, and H. Zhang, "Portable and wearable self-powered systems based on emerging energy harvesting technology," *Microsystems & Nanoengineering*, vol. 7, no. 1, pp. 1–14, 2021.
- [13] P. R. Adhikari, N. T. Tasneem, R. C. Reid, and I. Mahbub, "Electrode and electrolyte configurations for low frequency motion energy harvesting based on reverse electrowetting," *Scientific reports*, vol. 11, no. 1, pp. 1–13, 2021.
- [14] H. Yang, S. Hong, B. Koo, D. Lee, and Y.-B. Kim, "High-performance reverse electrowetting energy harvesting using atomic-layer-deposited dielectric film," *Nano Energy*, vol. 31, pp. 450–455, 2017.
- [15] H. Yang, H. Lee, Y. Lim, M. Christy, and Y.-B. Kim, "Laminated structure of al2o3 and tio2 for enhancing performance of reverse electrowetting-on-dielectric energy harvesting," *International Journal of Precision Engineering and Manufacturing-Green Technology*, vol. 8, no. 1, pp. 103–111, 2021.
- [16] T.-H. Hsu, S. Manakasettharn, J. A. Taylor, and T. Krupenkin, "Bubbler: a novel ultra-high power density energy harvesting method based on reverse electrowetting," *Scientific reports*, vol. 5, no. 1, pp. 1–13, 2015.
- [17] P. R. Adhikari, N. T. Tasneem, D. K. Biswas, R. C. Reid, and I. Mahbub, "Reverse electrowetting-on-dielectric energy harvesting integrated with charge amplifier and rectifier for self-powered motion sensors," in ASME International Mechanical Engineering Congress and Exposition, vol. 84560. American Society of Mechanical Engineers, 2020, p. V008T08A035.
- [18] J. H. Cho, G. Y. Kim, S. B. Choi, T.-j. Jeon, and S. M. Kim, "Micro energy harvesting system based on reverse electro wetting on dielectric (rewod)," *The KSFM Journal of Fluid Machinery*, vol. 18, no. 6, pp. 27–30, 2015.
- [19] P. R. Adhikari, R. C. Reid, and I. Mahbub, "High power density and bias-free reverse electrowetting energy harvesting using surface area

- enhanced porous electrodes," *Journal of Power Sources*, vol. 517, p. 230726, 2022.
- [20] M. B. Kulkarni and S. Goel, "Recent advancements in integrated microthermofluidic systems for biochemical and biomedical applications—a review," Sensors and Actuators A: Physical, p. 113590, 2022.
- [21] J. Lee, H. Moon, J. Fowler, T. Schoellhammer, and C.-J. Kim, "Electrowetting and electrowetting-on-dielectric for microscale liquid handling," Sensors and Actuators A: Physical, vol. 95, no. 2, pp. 259–268, 2002, papers from the Proceedings of the 14th IEEE Internat. Conf. on MicroElectroMechanical Systems. [Online]. Available: https://www.sciencedirect.com/science/article/pii/S0924424701007348
- [22] N. Weng, Q. Wang, J. Gu, J. Li, C. Wang, and W. Yao, "The dynamics of droplet detachment in reversed electrowetting (rew)," Colloids and Surfaces A: Physicochemical and Engineering Aspects, vol. 616, p. 126303, 2021. [Online]. Available: https://www.sciencedirect.com/science/article/pii/S0927775721001722
- [23] R. Rusev, G. Angelov, K. Angelov, and D. Nikolov, "A model for reverse electrowetting with cost-effective materials," in 2017 XXVI International Scientific Conference Electronics (ET), 2017, pp. 1–4.
- [24] P. R. Adhikari, A. Patwary, K. Kakaraparty, A. Gunti, R. C. Reid, and I. Mahbub, "Advancing reverse electrowetting-on-dielectric from planar to rough surface electrodes for high power density energy harvesting," *Energy Technology*, 2022.
- [25] K. Xiao and C.-X. Wu, "Dynamics of droplets driven by electrowetting," arXiv preprint arXiv:2203.12391, 2022.
- [26] N. T. Tasneem, D. K. Biswas, P. R. Adhikari, A. Gunti, A. B. Patwary, R. C. Reid, and I. Mahbub, "A self-powered wireless motion sensor based on a high-surface area reverse electrowetting-on-dielectric energy harvester," *Scientific Reports*, vol. 12, no. 1, pp. 1–15, 2022.
- [27] S. C. Chandrarathna and J.-W. Lee, "16.8 nw ultra-low-power energy harvester ic for tiny ingestible sensors sustained by bio-galvanic energy source," *IEEE Transactions on Biomedical Circuits and Systems*, 2021.